Ordering Dynamics in the Two-Dimensional Stochastic Swift-Hohenberg Equation

K.R. Elder,[1] Jorge Viñals,[2] and Martin Grant[1]
[1] *Department of Physics, McGill University, Rutherford Building, 3600 University Street, Montréal, Québec, Canada H3A 2T8*
[2] *Supercomputer Computations Research Institute, B-186, Florida State University, Tallahassee, Florida 32306-4052*
(Received 10 September 1991; revised manuscript received 25 November 1991)

Numerical and analytic techniques are used to study the roll patterns which appear following a convective instability as modeled by the Swift-Hohenberg equation. The results of this work reveal the presence of a disordered state and a quasiordered state at large and small noise strengths, respectively. The dynamical approach to these states is shown to be rapid in the former case and slow in the later. Both numerical and analytic calculations indicate that the slow dynamics can be characterized by a simple scaling relationship.

PACS numbers: 47.20.Ky, 05.40.+j, 47.20.Hw, 47.25.Qv

The onset and formation of roll patterns in Rayleigh-Bénard convection is a complex nonlinear process that has been examined extensively in recent years [1–10]. In a typical experiment, a quiescent conducting state is brought above the convective threshold giving rise to convective rolls of arbitrary orientation (in large aspect ratio systems). When all sources of fluctuations are small (let ϵ' denote their amplitude) and boundary effects are negligible, the subsequent evolution is achieved through the reorientation of the rolls and the elimination of defects. In what follows a numerical and analytic study of a simple model of this process, known as the Swift-Hohenberg (SH) equation, is presented for a large aspect ratio system. Our investigation reveals several interesting features of the SH equation, including the presence of a transition between an ordered state at small ϵ' (characterized by large regions of parallel convective rolls) to a disordered state at high ϵ'. Furthermore, it is shown that the dynamics at low ϵ' can be understood in terms of a dynamic scaling relationship similar to that encountered in domain growth phenomena [11].

The stochastic SH equation models the onset of Rayleigh-Bénard convection through a two-dimensional real order parameter field, ψ, which is commensurate with the convective rolls. It is derived from the fluid dynamics equations in the Bousinesq approximation in the limit of large Prandtl number. The dimensionless form of the equation is

$$\frac{\partial\psi(\mathbf{r},t)}{\partial t} = \left[\gamma^2 - \left(1+\nabla^2\right)^2\right]\psi(\mathbf{r},t) - \psi^3(\mathbf{r},t) + \eta(\mathbf{r},t), \tag{1}$$

where γ is a dimensionless control parameter, $\langle\eta(\mathbf{r},t)\eta(\mathbf{r}',t')\rangle = 2\epsilon'\delta(\mathbf{r}-\mathbf{r}')\delta(t-t')$ and ϵ' is the noise intensity. The salient feature of this equation with the appropriate boundary conditions is that its associated Lyapunov functional is minimized by a periodic function with a nonzero wave vector (i.e., $||\mathbf{k}_0|| \approx 1$) that corresponds to a convecting state comprised of a set of parallel rolls.

The intent of this work is to understand both the nature of this convecting state and how it is dynamically obtained from an initially unstable state (defined by $\psi = 0$). To further this goal Eq. (1) was numerically evaluated on a two-dimensional square grid at discrete time intervals. Euler's method was used to discretize the time derivative, while the discrete approximation used for the Laplacian operator included contributions from nearest and next-nearest neighbors. The maximum size of the grid spacing (Δx) is limited by the size of the convective rolls ($2\pi/k_0 \approx 2\pi$). A value of $\Delta x = \pi/4$ was selected to satisfy this constraint, while the time step (Δt) was chosen to be $\Delta t = 0.05$ to avoid numerical instabilities. Test runs with smaller grid spacings indicate that our results for the structure factor (to be defined below) near $k_0 = 1$ are insensitive to decreasing the grid size. The bulk of the calculations were performed on a grid of 512×512 nodes with periodic boundary conditions on ψ for $\epsilon = 0.0$, 0.05, and 0.075 [where $\epsilon = \epsilon'/(\Delta x)^2$] at $\gamma = 0.5$. All results were averages over 25 independent runs. Additionally, at the same γ, smaller systems (i.e., 256×256) were used to examine both the dynamics (at $\epsilon = 0.025$, 0.065, and 0.1) and stationary solutions (at a large number of values of ϵ ranging from 0.0 to 0.09). The initial condition for nonzero ϵ was chosen to be $\psi(\mathbf{r}, t=0) = 0$, whereas for $\epsilon = 0$ we chose $\psi(\mathbf{r}, t=0)$ to be a Gaussian random variable centered at zero of width 0.1.

The numerical results reveal a qualitative difference between the calculations performed at $\epsilon = 0.075$ and 0.1 from those at $\epsilon = 0.065$, 0.05, 0.025, and 0.0. A rapid (exponential) relaxation to the asymptotic stationary state was observed for the two largest values of ϵ while a slower (power law) evolution occurred at the smaller values of ϵ. The qualitative difference between the high and low ϵ runs is also apparent in the latest configurations. In Fig. 1 the one-point distribution function $\rho(\psi)$ is depicted for several values of ϵ at the latest times studied. The spherically averaged structure factor, $S(k,t) = \langle|\psi(k,t)|^2\rangle$, where k is the radial component of

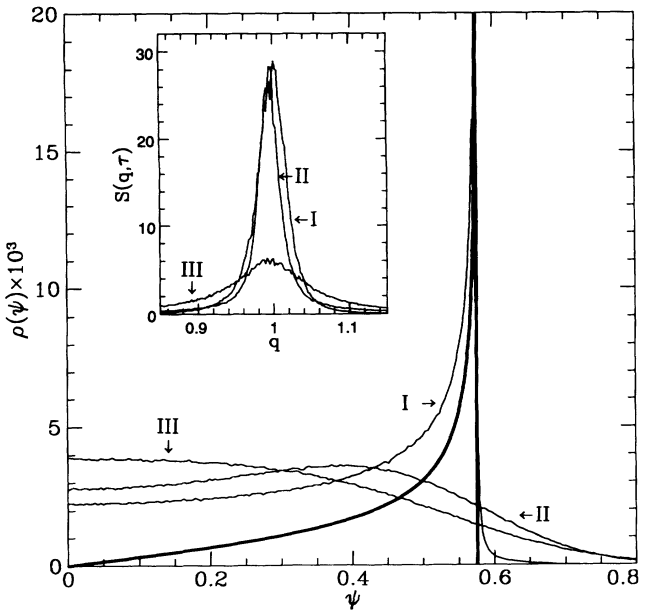

FIG. 1. One-point distribution function $\rho(\psi)$ and circularly averaged structure factor $S(k,t)$ (inset) obtained from a numerical solution of Eq. (1). The curves for $\epsilon = 0.0$, 0.05, and 0.075 are labeled I, II, and III, respectively. The thick solid line corresponds to a sine function.

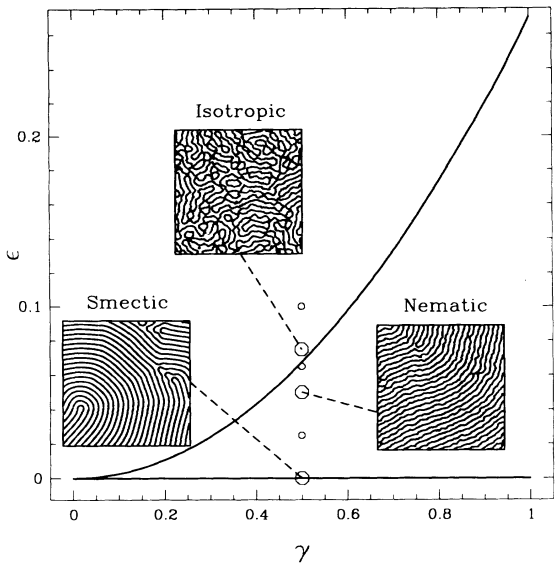

FIG. 2. Portions of size 100×100 of typical configurations obtained. The large and small circles correspond to the large and small (see text) numerical simulations conducted at $\epsilon = 0.075$, 0.05, and 0.0, and $\epsilon = 0.025$, 0.065, and 0.1, respectively. The configurations labeled isotropic, nematic, and smectic correspond to $\epsilon = 0.075$, 0.05, and 0.0, respectively. In all these plots the lines drawn are the lines of $\psi(\mathbf{r}) = 0$.

the wave vector, is shown at the same times in the inset of Fig. 1. For $\epsilon = 0.0$ and 0.05, Eq. (1) was solved for times up to $t = 10^4$, while for $\epsilon = 0.075$ the calculations were terminated at $t = 700$, since dynamical evolution past $t \approx 200$ was beyond numerical resolution [i.e., no further evolution of $S(k,t)$ and $\rho(\psi)$ could be distinguished past $t = 200$; one run was taken up to $t = 10^4$ for verification].

Figure 1 indicates that the latest configuration at $\epsilon = 0.075$ is characterized by a diffuse peak in the structure factor and a single peak in $\rho(\psi)$ centered at $\psi = 0$. In contrast, the latest configurations at $\epsilon = 0.05$ and 0.0, for example, had not reached a stationary state and gave rise to a sharp peak in $S(k,t)$ and a bimodal distribution in $\rho(\psi)$. The reason for the rapid relaxation to equilibrium at $\epsilon = 0.075$ is that the final state has a finite correlation length which is evident in the diffuse peak in $S(k,t)$. If an analogy with liquid crystals can be made, as suggested by Toner and Nelson [7,8], the various regimes can be identified as an *isotropic* regime with short-range order (for $\epsilon > \epsilon_{KT}$), a *nematic* or Kosterlitz-Thouless [12] regime with "quasi"-long-range orientational order (for $0 < \epsilon < \epsilon_{KT}$), and a *smectic* regime with long-range orientational and translational order (at $\epsilon = 0$). Portions of typical final configurations along with the phase diagram are shown in Fig. 2. Further indication of the transition at $\gamma = 0.5$ was obtained by first reaching a stationary solution at $\epsilon = 0.09$ and then decrementing ϵ in steps of 0.005 at time intervals of 10^3. The results of this study indicate that a transition [denoted by a sharp decrease in the peak in the structure factor and a crossover from a bimodal to unimodal distribution in $\rho(\psi)$] occurred in the interval $\epsilon_{KT} = 0.065 - 0.070$. It should be noted that while the numerical work was consistent with such a transition, it was not possible to distinguish between a transition from an isotropic to a translationally ordered state or from an isotropic to an orientationally ordered state.

The analysis of the dynamics below ϵ_{KT} is motivated by an approximate solution obtained by two of us [2] through a singular perturbation solution of Eq. (1), in which $S(k,t)$ was found to obey the following scaling relationship in the late-time, $k \approx 1$ limits:

$$S(k,t) = t^x f((k - k_0)t^x), \tag{2}$$

where x is a dynamic growth exponent and $f(z)$ is a scaling function. The implication of Eq. (2) is that all lengths (except for the convective roll width) should scale in time with the same dynamic exponent. With this in mind, several independent measures of length scales were calculated: the height (A), the width (w), and the first five moments of $S(k,t)$. A and w were obtained by fitting $S(k,t)$ by the form $Ae^{-[(k^2-k_0^2)/w]^2}$ (where $k_0 \approx 1$) and the moments m_n were defined to be $m_n(t) = \int_{k_0-w(t)}^{k_0+w(t)} dk|k - k_0|^n S(k,t)$. According to Eq. (2), $m_n(t) \propto t^{-nx}$, $w \propto t^{-x}$, and $A \propto t^x$. In Fig. 3 all measured quantities are displayed for $\epsilon = 0.05$. The corresponding exponents measured for these length scales were all within 1% of $\frac{1}{4}$. For $\epsilon = 0.0$ the exponents were all within 2% of $\frac{1}{5}$. The difference between the exponents

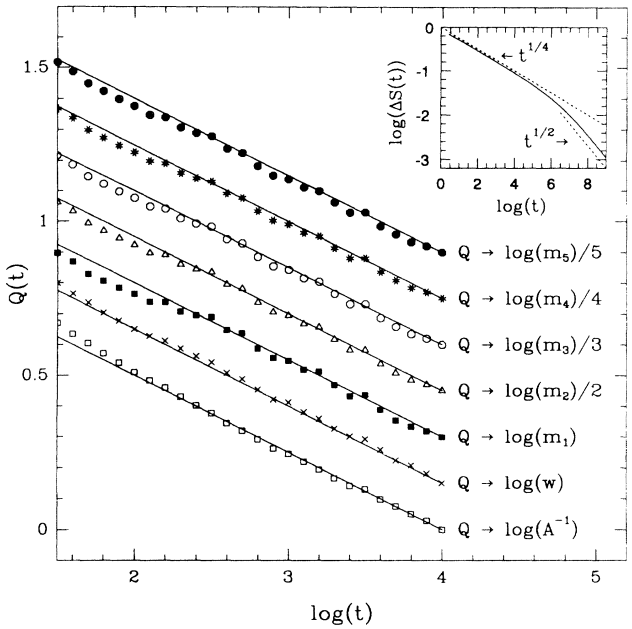

FIG. 3. Amplitude $A(t)$, width $w(t)$, and first five moments $m_n(t)$ of $S(k,t)$ as defined in the text displayed for $\epsilon = 0.05$. The solid lines are presented as guides to the eye and all have slope $x = \frac{1}{4}$. Inset: ΔS plotted on a logarithmic scale for $\gamma = 0.5$.

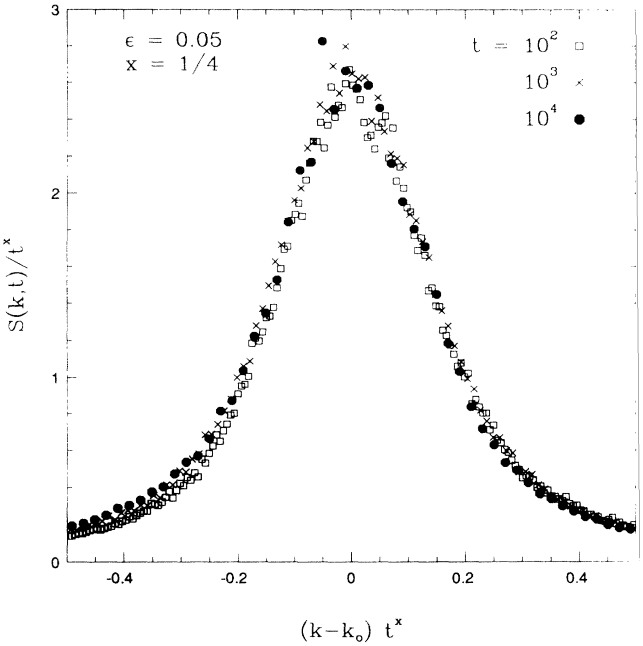

FIG. 4. The scaling property of the structure factor is illustrated by plotting $S(k,t)/t^{1/4}$ vs $(k-k_0)t^{1/4}$ at various times for $\epsilon = 0.05$. The open squares, crosses, and solid circles correspond to $t = 10^2$, 10^3, and 10^4, respectively.

obtained at $\epsilon = 0.05$ and 0.0 is most likely due to the difficulty in removing defects at $\epsilon = 0$ (visual examination of the configurations reveals a higher density of defects at $\epsilon = 0.0$). Equation (2) is further examined for $\epsilon = 0.05$ in Fig. 4, where $S(k,t)/t^x$ is plotted versus $(k-k_0)t^x$, at $t = 10^2$, 10^3, and 10^4. All curves overlap near $k = k_0$ when an exponent $x = \frac{1}{4}$ was used. Similar agreement was seen for $\epsilon = 0.0$ with $x = \frac{1}{5}$. Although the statistics collected for $\epsilon = 0.025$ and 0.065 were not sufficient to obtain accurate exponents, the measured exponents were much closer to $\frac{1}{4}$ than $\frac{1}{5}$.

The agreement of the exponents measured from the different lengths for $0 < \epsilon < \epsilon_{KT}$ is a strong indication that the dynamic scaling relationship is valid. The exponent obtained is, however, smaller than that anticipated in previous work (i.e., $x = \frac{1}{2}$) [2]. To address this discrepancy an alternative calculation is presented to investigate the possible existence of crossover effects in the absence of defects. To do so consider a set of parallel stripes the orientation of which varies slowly in space. The dynamics of such a configuration can be best studied by introducing a coordinate system that tracks the interface given by the spatial points at which $\psi = 0$. Specifically the Cartesian coordinates (x,y) are mapped onto orthogonal curvilinear coordinates (u,s), where u and s are locally normal and parallel to the lines $\psi(\mathbf{r},t) = 0$, respectively. By assuming that the stationary solution of the one-dimensional Swift-Hohenberg equation is a good approximation in the normal direction, and that the local curvature (κ) of the roll pattern is small (i.e., $\kappa/k_0 \ll 1$), Eq. (1) becomes

$$(\partial\psi^s/\partial u)(\partial u/\partial t) \approx -2\kappa(\partial\psi^s/\partial u + \partial^3\psi^s/\partial u^3) - \kappa_{ss}(\partial\psi^s/\partial u) + \eta\,, \tag{3}$$

where $\kappa_{ss} = \partial^2\kappa/\partial s^2$ and ψ^s is a solution of $\psi^s(u(\mathbf{r},t))^3 = [\gamma^2 - (1+\partial^2/\partial u^2)^2]\psi^s(u(\mathbf{r},t))$. Applying the projection operator, $\int_{-(\pi/2k_0)}^{(\pi/2k_0)} du(\partial\psi^s/\partial u)$, to Eq. (3) produces the following result:

$$v = -a\kappa + \kappa_{ss} - \zeta, \tag{4}$$

where $v = -\partial u/\partial t$, $a = -2(1+\beta/\sigma)$, $\sigma = \int du(\partial\psi^s/\partial u)^2$, $\beta = \int du(\partial\psi^s/\partial u)(\partial^3\psi^s/\partial u^3)$, $\langle\zeta\zeta'\rangle = \epsilon_I\delta(s-s') \times \delta(t-t')$, and $\epsilon_I = 2\epsilon'/\sigma$. The coefficient a and the interfacial noise amplitude ϵ_I can be estimated by using an approximate one-dimensional stationary solution derived by Pomeau and Manneville [6] which is valid in the limit of small γ. In this approximation a is extremely small ($a \approx 1.2 \times 10^{-4}$ for $\gamma = 0.5$), while $\epsilon_I = 3\epsilon'/2\pi\gamma^2$. The rolls will break apart when the interfacial noise amplitude is of the order of the roll width. Thus a transition to an isotropic state occurs when $\epsilon' \propto \gamma^2$.

A dimensional analysis of Eq. (4) reveals that the rolls relax asymptotically at a rate of $t^{-1/2}$, while at earlier times ($a^2t/2 < 1$) a smaller relaxation rate is expected. In the inset of Fig. 3 the deviations (ΔS) of the arc length from its asymptotic value are plotted for $\gamma = 0.5$, showing that a crossover from a relaxational rate of $t^{-1/4}$ to the asymptotic rate of $t^{-1/2}$ is expected to occur at $t \approx 10^5 - 10^7$. From this result it can be inferred that

a regime characterized by an effective exponent $x = \frac{1}{4}$ could be obtained for the first four or five decades in time, before taking on the asymptotic value of $x = \frac{1}{2}$. Despite this appealing interpretation of our numerical results it is important to emphasize that no numerical evidence for an asymptotic exponent of $x = \frac{1}{2}$ has been found, nor is there any evidence of crossover behavior [which would lead to nonscaling behavior in $S(k,t)$].

To recapitulate, the results of both numerical and analytic calculations indicate the presence of a transition between a quasiordered and an isotropic state, which are characterized by long- and short-range order, respectively. An independent estimate of the transition line ($\epsilon \propto \gamma^2$) was obtained from the interfacial calculation. In addition, dynamical scaling with a growth exponent of $x = \frac{1}{4}$ was observed in the nematic region. The value of x found disagrees with an earlier theoretical calculation and we have presented a possible resolution of the discrepancy. We are, however, unable to explain the smaller exponent of $x = \frac{1}{5}$ observed for $\epsilon = 0$. Although this work focused on the stochastic Swift-Hohenberg equation, we expect that both features discussed, namely, the existence of a transition between a quasiordered and a disordered state, and the asymptotic dynamical scaling behavior, are generic features of two-dimensional systems in which a finite wavelength is selected for the asymptotic ordered state. For example, recent experimental studies of electrohydrodynamic convection in nematic liquid crystals [13] have been able to detect and quantify the amplitude of the fluctuations before onset (fluctuations in simple liquids are believed to be too small to produce observable effects such as the ones presented here). Furthermore, since typical roll widths in these systems are of the order of microns, large aspect ratio samples are readily available. Experimental verification of the issues discussed in this paper seems therefore possible.

This international cooperation has been made possible by a grant from NATO within the program "Chaos, Order and Patterns; Aspects of Nonlinearity," Project No. CRG 890482. This work is also supported by the Natural Sciences and Engineering Research Council of Canada, les Fond pour las Formation de Chercheurs et l'Aide a la Recherche de la Province de Québec, and by the Supercomputer Computations Research Institute, which is partially funded by the U.S. Department of Energy Contract No. DE-FC05-85ER25000. All the calculations reported here have been performed on the 64k-node Connection Machine at SCRI. We thank Maxi San Miguel, Mike Kosterlitz, Bertrand Morin, and Emilio Hernández-García for useful discussions.

[1] J. Swift and P. C. Hohenberg, Phys. Rev. A **15**, 319 (1977).
[2] K. R. Elder and M. Grant, J. Phys. A **23**, L803 (1990).
[3] V. Steinberg, G. Ahlers, and D. S. Cannell, Phys. Scr. **T9**, 97 (1984).
[4] C. W. Meyer, G. Ahlers, and D. S. Cannell, Phys. Rev. Lett. **59**, 1577 (1987).
[5] H. Xi, J. Viñals, and J. D. Gunton, Physica (Amsterdam) **177A**, 356 (1991).
[6] Y. Pomeau and P. Manneville, J. Phys. (Paris), Lett. **40**, L609 (1979).
[7] D. R. Nelson, in *Phase Transitions and Critical Phenomena*, edited by C. Domb and J. L. Lebowitz (Academic, London, 1983), Vol. 7.
[8] J. Toner and D. R. Nelson, Phys. Rev. B **23**, 316 (1981).
[9] H. R. Schober, E. Allroth, K. Schroeder, and H. Muller-Krumbhaar, Phys. Rev. A **33**, 567 (1986).
[10] J. Viñals, E. Hernández-García, M. San Miguel, and R. Toral, Phys. Rev. A **44**, 1123 (1991).
[11] J. D. Gunton, M. San Miguel, and P. S. Sahni, in *Phase Transitions and Critical Phenomena*, edited by C. Domb and J.L. Lebowitz (Academic, London, 1983), Vol. 8.
[12] J. M. Kosterlitz and D. J. Thouless, J. Phys. C **6**, 1181 (1973).
[13] I. Rehberg, S. Rasenat, M. de la Torre, W. Schöpf, F. Hörner, G. Ahlers, and H. R. Brand, Phys. Rev. Lett. **67**, 596 (1991).